Acta Pharmacologica Sinica

www.nature.com/aps

BRIEF COMMUNICATION

Estrogen-dependent KCa1.1 modulation is essential for retaining neuroexcitation of female-specific subpopulation of myelinated Ah-type baroreceptor neurons in rats

Lu-qi Wang[1,2], Zhao Qian[1,3], Hai-lan Ma[1], Meng Zhou[1], Hu-die Li[1], Chang-peng Cui[1], Da-li Luo[2], Xue-lian Li[1] and Bai-yan Li[1]

Female-specific subpopulation of myelinated Ah-type baroreceptor neurons (BRNs) in nodose ganglia is the neuroanatomical base of sexual-dimorphic autonomic control of blood pressure regulation, and KCa1.1 is a key player in modulating the neuroexcitation in nodose ganglia. In this study we investigated the exact mechanisms underlying KCa1.1-mediated neuroexcitation of myelinated Ah-type BRNs in the presence or absence of estrogen. BRNs were isolated from adult ovary intact (OVI) or ovariectomized (OVX) female rats, and identified electrophysiologically and fluorescently. Action potential (AP) and potassium currents were recorded using whole-cell recording. Consistently, myelinated Ah-type BRNs displayed a characteristic discharge pattern and significantly reduced excitability after OVX with narrowed AP duration and faster repolarization largely due to an upregulated iberiotoxin (IbTX)-sensitive component; the changes in AP waveform and repetitive discharge of Ah-types from OVX female rats were reversed by G1 (a selective agonist for estrogen membrane receptor GPR30, 100 nM) and/or IbTX (100 nM). In addition, the effect of G1 on repetitive discharge could be completely blocked by G15 (a selective antagonist for estrogen membrane receptor GPR30, 3 μM). These data suggest that estrogen deficiency by removing ovaries upregulates KCa1.1 channel protein in Ah-type BRNs, and subsequently increases AP repolarization and blunts neuroexcitation through estrogen membrane receptor signaling. Intriguingly, this upregulated KCa1.1 predicted electrophysiologically was confirmed by increased mean fluorescent intensity that was abolished by estrogen treatment. These electrophysiological findings combined with immunostaining and pharmacological manipulations reveal the crucial role of KCa1.1 in modulation of neuroexcitation especially in female-specific subpopulation of myelinated Ah-type BRNs and extend our current understanding of sexual dimorphism of neurocontrol of BP regulation.

Keyword: baroreflex afferent function; neuroexcitation; nodose ganglia; estrogen membrane receptor GPR30; KCa1.1; IbTX; G1; G15; whole-cell recording

Acta Pharmacologica Sinica (2021) 42:2173–2180; https://doi.org/10.1038/s41401-021-00722-4

INTRODUCTION

It has well been documented that the lower blood pressure (BP) and incidence of hypertension are more common in premenopausal females compared with that in age-matched males [1–4] and this gender-related difference disappears at post-menopausal when estrogen support is not available [2, 5, 6]. Fortunately, this puzzle has gradually been unmasked until the fact has firstly been reported by Li and Schild [7–11] regarding the female-specific distribution of myelinated Ah-type baroreceptor neurons (BRNs) in the nodose ganglia (NG) of adult female rats, rather than an age-matched male, through a series of experiments by using whole-cell patch technique with unique NG slice preparation [8] conjugated with immunohistochemical and pharmacological approaches. Most importantly, the neuronal excitability of Ah-type neurons relies largely on the presence of estrogen [10, 12–14] and the functional changes of this category neurons closely impact upon several clinical issues related to visceral/baroreflex afferent function such as hypertension [15–20], salient angina [21], asthma [22, 23], and so on. Accumulated evidences have demonstrated that KCa1.1 (BK-type Ca^{2+}-activated K^+ channel) plays a crucial role in neuroexcitation of central [24, 25], peripheral [26], and visceral sensory nervous system [12, 27–30] including baroreflex afferents except for Nav1.9 [31] and HCN1 [32], and KCa1.1-mediated neuroexcitation in NG neurons is closely associated with estrogen [10, 12]. Clearly, accumulated BK channel inactivation causes Ah-types to become more excitable [28] by means of frequency/use-dependent prolongation of action potential duration (APD_{50}) [29]. Additionally, by co-localization of HCN1 and KCa1.1, it has been found that KCa1.1 could be a unique marker for identification of Ah-type BRNs in the NG and Ah-type baroreceptive neurons in the NTS combined with the sensitivity to capsaicin [29, 30, 33]. Obviously, KCa1.1 is a major ion channel to retain the neuronal excitability of Ah-type neurons and a direct cause for sexual-related autonomic control of BP regulation and

[1]Department of Pharmacology, State-Province Key Laboratories of Biomedicine-Pharmaceutics of China, and Key Laboratory of Cardiovascular Medicine Research, Ministry of Education, College of Pharmacy, Harbin Medical University, Harbin 150081, China; [2]Department of Pharmacology, School of Basic Medical Sciences, Capital Medical University, Beijing 100069, China and [3]Department of Pharmacy, the First Affiliated Hospital of Harbin Medical University, Harbin 150010, China
Correspondence: Xue-lian Li (lixuelian@hrbmu.edu.cn) or Bai-yan Li (liby@ems.hrbmu.edu.cn)
These authors contributed equally: Lu-qi Wang, Zhao Qian.

Received: 24 February 2021 Revised: 20 June 2021 Accepted: 21 June 2021
Published online: 15 July 2021

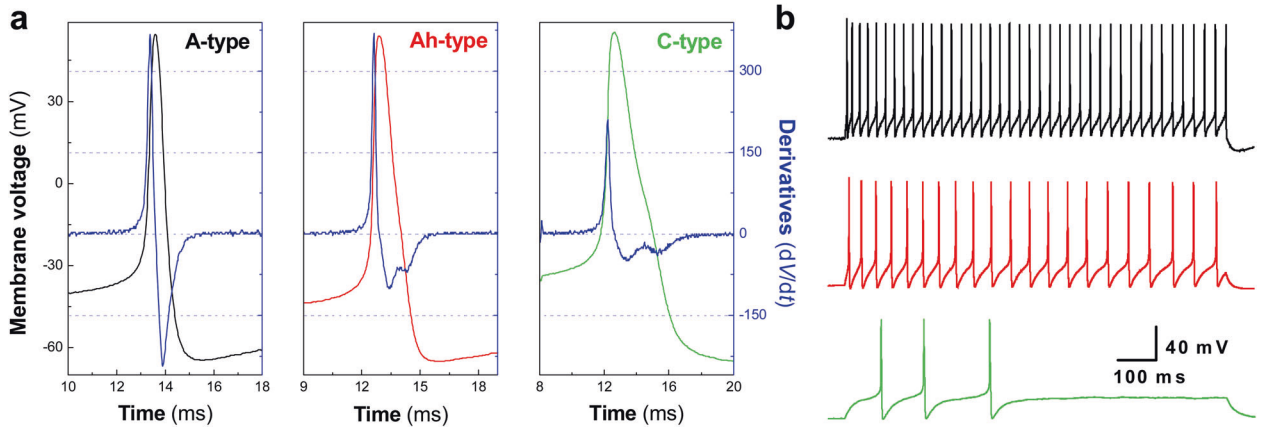

Fig. 1 Electrophysiological validation of neurons isolated from adult female rats Representative action potential (AP) and repetitive firings of same fluorescently and electrophysiologically identified myelinated A-, Ah-, and unmyelinated C-type baroreceptor neurons (BRNs) isolated from adult ovary intact (OVI) female rats. Single AP was elicited by brief pulse and the AP waveform parameters such as AP firing threshold (APFT), AP duration (APD_{50}), maximal up- (UV_{MAX}) and down-stroke velocity (DV_{MAX}) were collected for identification of afferent fiber types; repetitive discharge was also elicited by current-step depolarization to determine the firing frequency. **a** AP recordings from identified A- (left, black), Ah- (center, red), and C-type (right, green) BRNs and the derivatives over the membrane voltage created from each representative AP (blue, the current change as function over the membrane potential); **b** Repetitive firings from each corresponding AP shown in **a**. The scale bars were applied for all step recordings.

visceral afferent-related diseases in clinics. However, the underlying ion channel mechanism insight into the neuroexcitability has largely been unknown yet. In this regard, AP and repetitive discharge as well as voltage-gated K^+ currents were recorded using whole-cell patch technique and the changes in the neuroexcitability of identified Ah-type BRNs with/without estrogen support were evaluated before and after estrogen membrane receptor GPR30 modulation and/or KCa1.1 inactivation.

MATERIALS AND METHODS

Animals

Adult female Sprague-Dawley (SD) rats weighing 200–240 g were purchased from Animal Center of the Second Hospital, Harbin Medical University (SCXK (Hei) 2019-001). The rats were housed in a specific pathogen-free facility with 5 rats per cage and maintained at 23–25 °C with 12 h light–12 h dark cycle and standard rodent diet and water ad libitum. All protocols regarding animals used for electrophysiological recordings and immunohistochemical analysis were pre-approved by Institutional Animal Care and Use Committee of Harbin Medical University, which are in accordance with the recommendations of the Panel on Euthanasia of the American Veterinary Medical Association and the National Institutes of Health publication "Guide for the Care and Use of Laboratory Animals (http://www.nap.edu/readingroom/books/labrats/)."

Isolated neuron preparation

The procedures for isolated neuron from adult rats were described in detail previously [8, 9]. Briefly, the acutely isolated neurons from adult OVI or OVX female rats were cultured for at least 4 h before recording for ion channel recovery from enzymatic treatment and all recordings were completed within 6–10 h after isolation.

BRNs identification

BRNs were identified fluorescently followed by the procedures that were described previously [11, 34]. Briefly, the rats (75–100 g) were relaxed accordingly and left side aortic depressor nerve (ADN) was dissected very carefully and labeled with fluorescent dye (Dil, Molecular Probe, Thermo Fisher Scientific, Waltham, MA, USA), in which the Dil was sealed exactly by using silicon (medical grade for dentistry) on the ADN to avoid contamination of the Vagus. This process would ensure Dil-positive neurons are those that received the visceral inputs from baroreceptor terminals at aorta. The labeling procedures took place at least one week before the acute isolation that would leave enough time for the Dil to be transported to the nodose ganglion (left) along with axon. For isolation, the left side nodose ganglion was dissected and isolated enzymatically and the fluorescent-positive neurons were considered as BRNs.

Afferent fiber identification

The AP waveform parameters and repetitive discharge characteristics were obtained from the AP elicited by a brief pulse and current step depolarization, respectively. For afferent fiber type (neuron type) identification in isolated neurons, combined use of AP duration (APD_{50}), maximal up-stroke velocity (UV_{MAX}), maximal down-stroke velocity (DV_{MAX}), and the repolarization hump was applied [7]. In some cases, morphological [11] and pharmacological approaches [9] were also selected for further confirmation. For myelinated A-types (Fig. 1a, left): APD_{50} is absolutely less than 1.0 ms with highest repetitive firing (Fig. 1b, upper panel) and fast UV_{MAX} and DV_{MAX} without repolarization hump; for myelinated Ah-types (Fig. 1a, center): APD_{50} is always between 1–2 ms with repolarization hump, and UV_{MAX} and DV_{MAX} are over 250 mV/ms and 75 mV/ms, respectively; for unmyelinated C-types (Fig. 1a, right): APD_{50} is always beyond 2.0 ms with significant repolarization hump, and UV_{MAX} and DV_{MAX} are never over 250 mV/ms and 75 mV/ms. Additionally, the frequency of repetitive discharge would be another factor to identify myelinated Ah- and unmyelinated C-types (Fig. 1b, center and lower panels).

Whole-cell patch technique and recording solutions

The protocols for both current- and voltage-clamp recordings were described in details as previously [29]. IbTX-sensitive component (presumably KCa1.1) was obtained by subtraction of total outward K^+ current in the presence of 100 nM IbTX (Alomone Lab, Jerusalem, Israel, applied by microperfusion) from that without IbTX. The formulas for both pipette (intracellular) and bath (extracellular) solutions used in this experiment were identical to those described previously [10]. For intracellular solution (in mM): (i) for AP recording, 6 NaCl, 50 KCl, 50 K_2SO_4, 5 $MgCl_2$, and 10 HEPES; (ii) for K^+ channel recording, 137 NMDG, 5.4 KCl, 1.0 $MgCl_2$, 10 glucose, and 10 HEPES. For extracellular solution (in mM): (i) for AP recording, 137.0 NaCl, 5.4 KCl, 1.0 $MgCl_2$, 10 glucose, and 10 HEPES; (ii) for K^+ channel recordings: 140 K-

Table 1. Effects of 100 nM iberiotoxin (IbTX) on action potential and repetitive discharge of identified baroreceptor neurons (BRNs) isolated from adult ovary intact (OVI) female rats.

	Myelinated Ah-type baroreceptor neurons	
	Control	100 nM IbTX
Brief pulse-evoked single AP		
APD_{50}	1.78 ± 0.28	2.12 ± 0.34**
DV_{MAX}	−104.7 ± 17.6	−77.3 ± 11.2*
Step current-elicited repetitive discharge		
10 pA	0.0 ± 0.00	1.28 ± 0.13*
30 pA	2.18 ± 0.2	6.66 ± 1.05**
60 pA	6.45 ± 1.67	12.2 ± 2.53**

Note: APD_{50}: action potential duration measured at 50% height amplitude (ms); DV_{APDMAX}: maximal down-stroke velocity (derivative: d*V*/d*t*, mV/ms)
Single action potential (AP) was evoked by a brief pulse to quantify the afferent fiber type and repetitive discharge was elicited by current step depolarizations (10, 30, and 60 pA) initiated from below threshold to superthreshold levels before and after 100 nM of IbTX. Averaged data were expressed as mean ± SD, $n = 6$ complete recordings from 4 rats. *$P < 0.05$ and **$P < 0.01$ vs. control.

Aspartate (K-ASP), 3 $MgCl_2$, and 10 HEPES. The pH for extracellular and intracellular solutions was adjusted to 7.30 and 7.20, respectively. D-Manitol was used to adjust osmolarity for extracellular and intracellular solutions to 310 and 290, respectively. Raw data were low-pass filtered to 10 kHz and digitized at 50 kHz. All experimental protocols, data collection and preliminary analysis were carried out using pCLAMP 10 and the Digidata 1440 (Molecular Devices, San Jose, CA, USA) operated on a PC platform.

Immunochemical fluorescent analysis

The tissue collection, preparation, and staining procedures as well as analysis were followed up by the protocols exactly as described previously [15, 30].

Data acquisition and statistical analysis

Data for whole-cell recordings were obtained by using Clampex and analyzed using Clampfit (Molecular Devices; Sunnyvale, CA, USA). Excel and Origin (Microsoft, Northampton, PA, USA) were used for data analysis and figure graphing, respectively. Image-pro plus (Media Cybernetics, MD, USA) was used for fluorescent intensity analysis. Un-paired and paired Student's *t* tests were applied for the difference between groups or before and after treatment. One-way ANOVA with post-hoc Turkey test was also applied where appropriated. The number (*n*) of the test represents the complete recording from neurons from at least three rats. Averaged data were expressed as mean ± SD and the *P* value less than 0.05 was considered as statistical significance.

RESULTS

Functionally upregulated neuroexcitation by inactivation of KCa1.1

To verify the KCa1.1-mediated neuroexcitation, AP waveform parameters and discharge characteristics of identified myelinated Ah-type BRNs isolated from OVI female rats were evaluated (Table 1). Consistently, in the presence of 100 nM IbTX, APD_{50} was increased ($P < 0.01$) and DV_{MAX} was reduced ($P < 0.05$) compared with control. Under the same experimental condition, the frequency of repetitive firing elicited by a series of current step depolarizations (10, 30, and 60 pA) was also enhanced significantly ($P < 0.05$ or $P < 0.01$ vs. control) by 100 nM IbTX. These results demonstrate that Ah-type BRNs functionally express KCa1.1 and their excitability could be upregulated by KCa1.1 inactivation.

Faster AP repolarization and blunt repetitive firing of Ah-type BRNs in the absence of estrogen

Our previous recordings have shown that OVX procedure accelerates the rate of repolarization and reduces APD_{50} as well as fails to elicit the repetitive firings [23], and this alternation of waveform and neuronal excitability of Ah-type visceral afferent neurons (general population, without known afferent modality) could be reversed in the presence of estrogen concentration dependently [10]. In the current observations, all rats underwent procedures of aortic depressor nerve (ADN) DiI labeling and all recordings were collected from fluorescently and electrophysiologically identified BRNs (known afferent modality/baroreceptor and fiber type). As expected, similar results were recorded in these Ah-type BRNs isolated from OVX female rats. As compared with OVI female rats (Fig. 2a), the repolarization was significantly increased with correspondent brief APD_{50} that was shortened by up to ~30% (Fig. 2a), the total outward current illustrated by the phase plots during repolarization (positive portion of derivative) was almost doubled (Fig. 2b) without marked change in total inward current (negative portion of derivative), and tested Ah-type BRNs failed to fire AP repetitively (Fig. 2c).

Upon the faster rate of repolarization compared with OVI, functionally upregulated KCa1.1 channels are more conspicuous in the absence of estrogen [12]. In this regard, total outward K^+ currents were obtained from identified BRNs of both OVI and OVX female rats before and after 100 nM IbTX under voltage-clamp configuration. The results showed that the current density of total outward K^+ currents were obviously increased in Ah-types of OVX compared with those of OVI female rats and this functional upregulation of K^+ was largely attributed as the proportional increase in IbTX-sensitive component (Fig. 2d–g).

Estrogen-dependent KCa1.1 channel modulation observed only in Ah-type BRNs

Clear evidences from our previous observation have shown that the neuroexcitability of myelinated A-, Ah-, and unmyelinated C-type visceral afferent neurons from OVI female rats are not influenced by estrogen [10, 23]. Similarly, the AP waveform and repetitive discharge in A- and C-type BRNs were not significantly altered before and after OVX procedure (data not shown), except for female-specific subpopulation of Ah-types. However, reduced neuroexcitability of Ah-types isolated from OVX female rats was completely restored by estrogen via its receptor-β, rather than receptor-α [10]. To avoid a wide variety of physiological action mediated presumably in the presence of estrogen, G1, a specific agonist for GPR30 (membrane receptor of estrogen), was selected in the current observation. The results showed that APD_{50}, DV_{MAX}, and AP firing frequency (APFF) of Ah-type BRNs from OVI female rats (Fig. 3a, c) were slightly but not significantly changed in the presence of 100 nM G1. However, both APD_{50} and DV_{MAX} were altered markedly in the Ah-types isolated from OVX female rats ($P < 0.05$ vs. OVI) by 100 nM G1 without further change by IbTX on top of G1 (Fig. 3b). Obviously, Ah-type BRNs from OVX females failed to fire AP repetitively (Fig. 3d, upper panel) and this reduced neuroexcitability was completely reversed by 100 nM G1 (Fig. 3d, center panel) without any further increase in the firing frequency by additional 100 nM IbTX on top of G1 (Fig. 3d, lower panel). These observations imply that lack of estrogen support would functionally upregulate KCa1.1 and subsequently downregulate neuroexcitation of Ah-types; in other words, estrogen plays a critical role in maintaining the neuroexcitability of Ah-type BRNs by negative regulation of KCa1.1 functional expression and this effect of estrogen could be mimicked by its membrane receptor GPR30 activation.

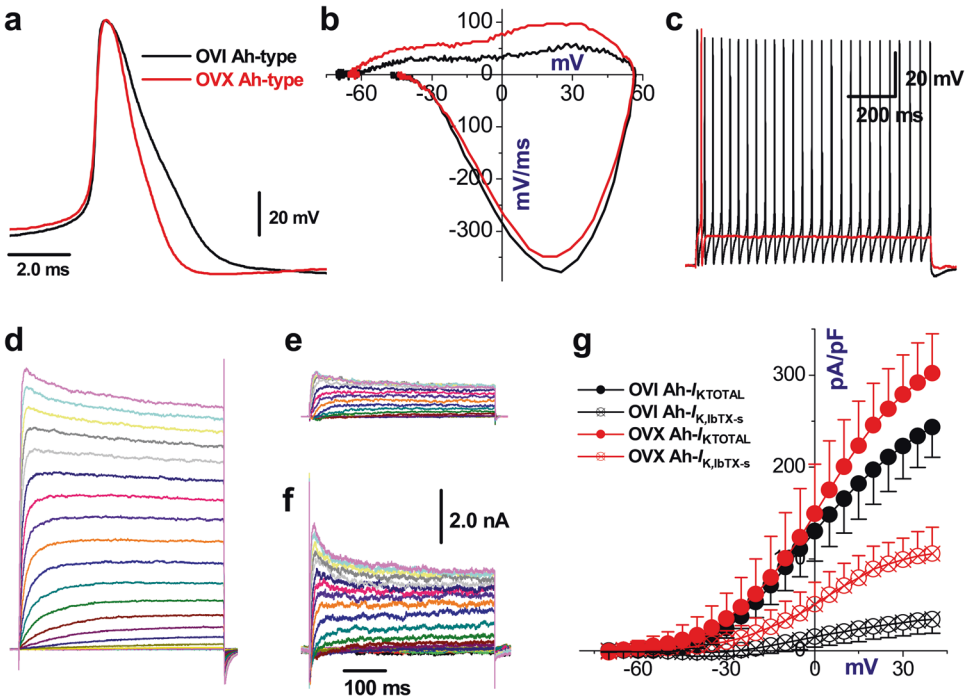

Fig. 2 Changes in AP waveform characters of Ah-type BRNs isolated from OVI and OVX female rats and effect of IbTX on K^+ channel currents. Ovariectomy (OVX) upregulates the iberiotoxin-sensitive (IbTX-s) component of K^+ currents recorded from identified myelinated Ah-type BRNs compared with ovary intact (OVI) female rats. Single AP was collected firstly for afferent fiber type classification and followed by voltage-clamp recording before and after 100 nM IbTX by microperfusion, in which the cell was held at −80 mV and stepped from −70 mV to +40 mV with 5 mV increment for 450 ms, the interpulse interval is 1.0 s. **a**, **b** The superimposition of AP and derivative current changes during AP recorded from OVI (black) and OVX (red) female rats, respectively. **c** Repetitive firings of same neurons in **a**. **d** Representative total outward K^+ currents (I_{KTOTAL}) from OVI female rats. **e**, **f** IbTX-s components from OVI and OVX female rats, respectively. **g** The current–voltage relationship (*I–V* curves) of total outward K^+ current (I_{KTOTAL}) and iberiotoxin (IbTX)-sensitive ($I_{K,\ IbTX-s}$) components of myelinated Ah-type BRNs from OVI and OVX female rats. Average data were presented as mean ± SD, $n = 7$ complete recordings from 5 and 4 rats for OVI and OVX, respectively. $P < 0.01$ vs. OVI. Scale bars in **f** were applied for all voltage-clamp recordings

Effect of G1 on repetitive discharge capability upon the initial discharge frequency and stimulus intensity of current-step depolarization

In order to compare the difference in the frequency of repetitive discharge of Ah-type BRNs isolated from OVI and OVX female rats, the superthreshold stimulus intensity (120 pA step depolarization) was selected, which may elicit a saturate repetitive discharge in Ah-types and the effect of G1 on APFF may not be observed clearly with this stimulus intensity. For this regard, a series of stimulus intensity of current-step depolarization (20, 30, and 60 up to 120 pA) was applied in the following test (Table 2). The results indicated that 20 pA step almost did not elicit repetitive firings in majority of Ah-type BRNs (Fig. 1a, upper panel) in stark contrast to 120 pA step depolarization (Fig. 3c); the frequency of repetitive firings was significantly increased under all applied stimulation in the presence of 100 nM G1 (Table 2; Fig. 4a, b, center panels). Intriguingly, the most dramatic effect of G1 on the frequency of repetitive discharge was observed under 20 pA step depolarization. The estimated increase in the percentage (%) of firing frequency was ~490% and this increased firing frequency declined in a stimulus intensity-dependent fashion (Table 2). Apparently, 120 pA step depolarization elicited almost saturation. No matter what stimulus intensity, G1-induced increase in the frequency of repetitive discharges was completely abolished by 3 μM G15, a specific antagonist for GPR30 (Fig. 4a, b, lower panels). These data strongly suggest that the effect of G1 on the frequency of repetitive firing is closely associated with the initial status of repetitive discharge elicited by current-step depolarization. Additionally, the data from the tests with G15 further confirm that estrogen-dependent KCa1.1 modulation plays a vital role in the neuroexcitation of Ah-type BRNs and female- and afferent-specific baroreflex modulation of BP, which is a presumably major factor to retain relatively lower BP in adult OVI female rats.

Unique distribution of KCa1.1 protein in Ah-type BRNs

Our previous immunohistochemical observation has demonstrated that strong immunofluorescence against KCa1.1 is only detected in IB4-positive (presumably unmyelinated afferents) neurons [28] when using adult male rats, which is supported by the electrophysiological data that AP discharge characters of myelinated A-types are not modified by charybdotoxin and IbTX [35]. Even though mRNA for KCa1.1 can be detected in myelinated A-type cells isolated from adult male rats [33], a strong immunofluorescence against KCa1.1 is not detected in all IB4-negative (presumably myelinated afferents) neurons in adult male rats. Conjugated with current electrophysiological data, we have a strong reason to hypothesize that immunofluorescence is likely to be observed in myelinated Ah-type BRNs isolated from adult OVI female rats. The current immunostaining data (Fig. 5) indicated that fluorescence was detected in clustered IB4-negative and KCa1.1-positive neurons of adult OVI female rats. The mean fluorescent intensity of IB4-negative (Fig. 6a), rather than IB4-positive group (Fig. 6b), was markedly enhanced in OVX female group and this enhancement of fluorescence was reversed in OVX female rats with estrogen (E_2) treatment for 4 weeks after OVX procedure, suggesting estrogen-mediated

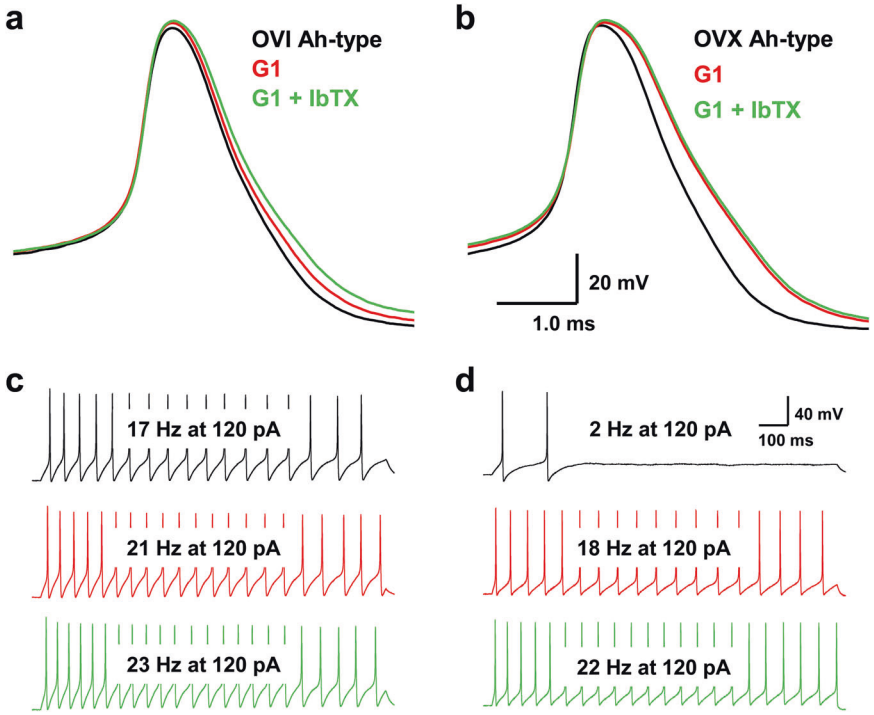

Fig. 3 Changes in the trajectory of AP and discharge profiles in myelinated Ah-type BRNs isolated from OVI and OVX female rats before and after 100 nM G1 (selective agonist for estrogen membrane receptor GPR30) or G1 + 100 nM IbTX. The same pulse and step depolarization were applied before and after tests. **a**, **b** Representative AP recorded from identified Ah-type BRNs isolated from OVI and OVX female rats in the absence and presence of G1 or G1 + IbTX, respectively, under same brief pulse. **c**, **d** Representative recordings of repetitive discharge elicited by identical step-depolarization (120 pA) from same Ah-type BRNs of OVI and OVX female rats before and after G1 or G1 + IbTX treatments. The scale bars shown in **d** were applied for all step recordings.

Table 2. The effects of G1, a selective agonist of GPR30, and G15, a selective antagonist of GPR30, on the repetitive discharge in identified myelinated Ah-type baroreceptor neurons (BRNs) isolated from adult ovary intact female rats.

Current-step depolarization (pA)	Control	G1 100 nM (%)	G1 + G15 3.0 μM
20	0.76 ± 0.33	4.51 ± 1.44 (~ 490)**	0.85 ± 0.57††
30	3.04 ± 0.86	9.44 ± 4.18 (~ 210)**	2.91 ± 1.06††
60	6.5 ± 2.3	12.5 ± 3.4 (~ 92)**	5.8 ± 3.8††
120	16.7 ± 4.4	20.2 ± 5.08 (~ 21)*	15.9 ± 4.6†

In this study, a single action potential (AP) is recorded routinely using a brief current pulse delivered to soma directly by recording electrode, which provides AP parameters and additional quantification for derivative change over the membrane potential to classify afferent fiber types upon the standard validation. On the same neuron, the current-step depolarization ranging from near threshold up to superthreshold is also delivered to soma before and after 100 nM G1 or G1 + 3.0 μM G15 to quantify the changes in repetitive discharge frequency at different levels of current-step depolarization. Additionally, G1-mediated increased percentage (%) of repetitive firing frequency was also estimated. Averaged data were expressed as mean ± SD, $n = 5$ complete recordings from 3 rats. *$P < 0.05$ and **$P < 0.01$ vs. control, $^{\dagger}P < 0.05$ and $^{\dagger\dagger}P < 0.01$ vs. G1.

downregulation of KCa1.1 channel protein leading to the restoration of neuroexcitability.

DISCUSSION

Electrophysiological conjugated with pharmacological data collected from current observation have provided additional evidence that KCa1.1 channel is a crucial player in modulation of neuroexcitation especially in the female-specific subpopulation of myelinated Ah-type BRNs and extend our current understanding of sexual dimorphism of neurocontrol of BP regulation through baroreflex afferent pathway.

Even though the electrophysiological and pharmacological validations conjugated with Dil labeling technique could precisely identify and classify the myelinated Ah-types isolated from adult female rats, the immunohistochemical analysis using specific antibody is worthy of doing because a direct visualization of cell classification upon protein expression could be done and may provide further evidence to support electrophysiological data. One technical limitation remains that by co-localization of IB4 and KCa1.1 we could not exactly distinguish myelinated A-type from Ah-type neurons in current condition; however, calculated mean fluorescent intensity among OVI, OVX, and OVX plus E_2 groups is overlaid in a larger population of neurons, suggesting that the fluorescence intensity of these grouped neurons may not be changed while lacking estrogen support or the treatment of OVX with estrogen because they are likely a myelinated A-types and KCa1.1 does not play a role in the excitability in A-types even though the mRNA for KCa1.1 α- and β4-subunits could be detected [33]. Interestingly, double negative neurons against both

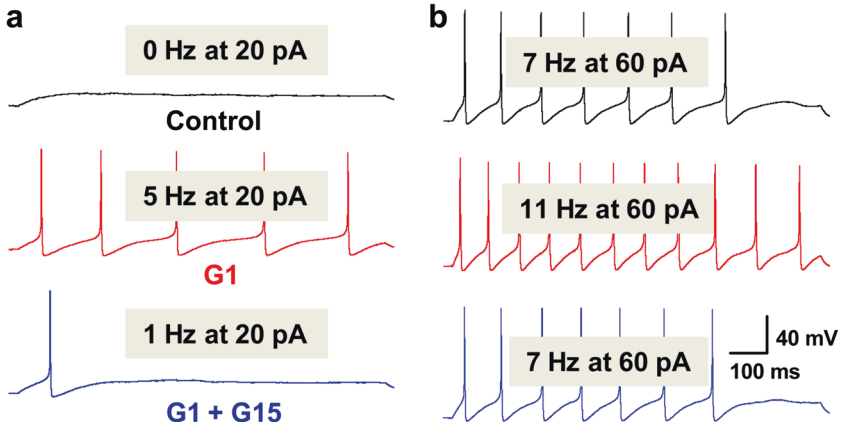

Fig. 4 Changes in repetitive discharge in the absence or presence of G1 100 nM or G1 + 3 μM G15 (selective antagonist for estrogen membrane receptor GPR30). a The repetitive firings were evoked by 20 pA (sub-threshold stimulation) before and after treatments. **b** The repetitive firings were evoked by 60 pA step depolarization (superthreshold stimulation) before and after treatments. The scale bars shown in **b** were applied for all step recordings.

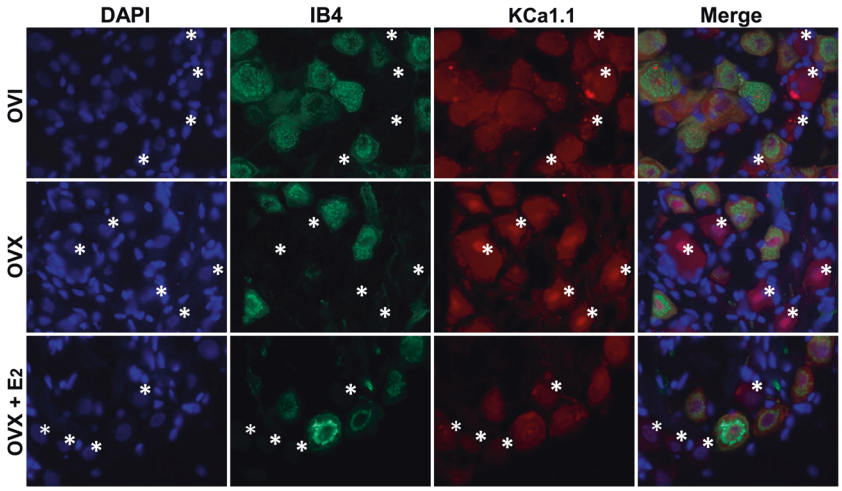

Fig. 5 Immunohistochemical analysis of KCa1.1 in Ah-type BRNs of OVI, OVX female rats, and OVX treated with estrogen. Immunohistochemical co-localization of isolectin B4 (IB4) and KCa1.1 to verify the changes in the mean fluorescent density of identified myelinated Ah-type BRNs in tissue level of nodose ganglia from OVI, OVX, and OVX female rats treated with estrogen (E_2) for 4 weeks after OVX procedure. IB4-positive neurons are presumably unmyelinated C-types. Both negative for IB4 and KCa1.1 are presumably myelinated A-types. IB4-negative but KCa1.1-positive neurons (indicated by white asterisks) are presumably myelinated Ah-types neurons.

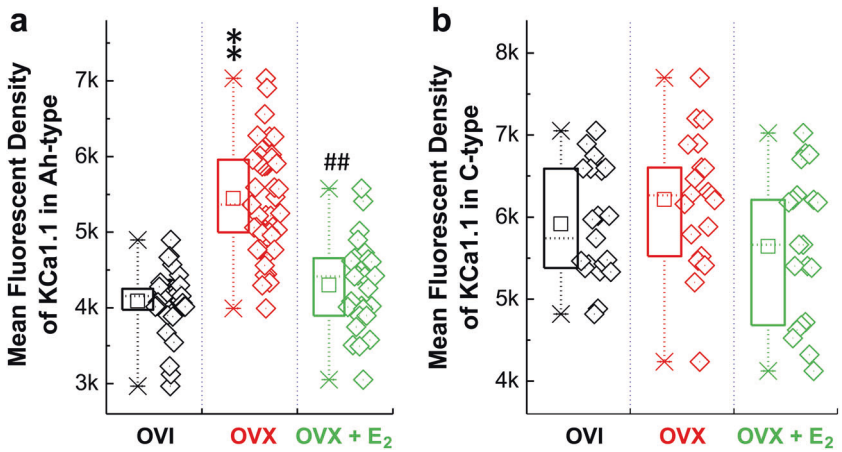

Fig. 6 The averaged changes in the mean fluorescent density of identified BRNs from the tissue level of nodose ganglia of OVI, OVX, and OVX female rats treated with E_2 for 4 weeks after OVX procedure. a Identified myelinated Ah-type BRNs. **b** Identified unmyelinated C-type BRNs. Averaged data were presented as mean ± SD, and $n = 39$ for OVI, 49 for OVX, and 27 for OVX + E_2 in the category of Ah-types, $n = 20$ for OVI, OVX, and OVX + E_2, respectively, in the category of C-types. The data points (n) from each group were collected from at least 6 rats. $^{**}P < 0.01$ vs. OVI, $^{\#\#}P < 0.01$ vs. OVX.

IB4 and KCa1.1 with DAPI positively labeled were indeed observed in the preparation of adult male [28] or female rats (data not shown), suggesting that negative expression of KCa1.1 in certain myelinated neurons existed and this grouped neurons is supposed to be myelinated A-types.

Afterhyperpolarization including both fast and slow components is another ion channel mechanism to control AP firing rate/discharge frequency, which was not altered in identified Ah-types BRNs in the presence of IbTX observed in our previous report [32] except for AP duration, implying that afterhyperpolarization is not a key contributor in estrogen- and KCa1.1-mediated changes in neuroexcitation.

CONCLUSION

Taken all these data together, estrogen-dependent lower expression profile of KCa1.1 plays a key role in retaining the higher neuroexcitability of female-specific subpopulation of myelinated Ah-type BRNs in ovary-intact female rats, which is a perfect explanation why reduced neuroexcitability is observed in this category of BRNs through upregulation of KCa1.1 while losing estrogen support. Most importantly, this finding not only confirms the cellular basis of female-specific distribution of myelinated Ah-type BRNs but also explains the ion channel mechanism of estrogen-dependent KCa1.1 modulation insight into the sexual dimorphism of neurocontrol of BP regulation via baroreflex afferent pathway under physiological and pathophysiological condition.

ACKNOWLEDGEMENTS

This research was funded by National Natural Science Foundation of China (31171122, 81573431, and 81971326) to BYL.

AUTHOR CONTRIBUTIONS

LQW, ZQ, and BYL designed the study, conducted patch recording, and interpreted observation. HLM, MZ, HDL, and CPC performed ovariectomized surgery, neurons isolation, and immunostaining, prepared recording solution, and statistical evaluation. DLL, XLL, and BYL draft and revised the manuscript. ZQ, XLL, and BYL finalized the manuscript. BYL provided research funding.

ADDITIONAL INFORMATION

Competing interests: The authors declare no competing interests.

REFERENCES

1. Guzik P, Schneider A, Piskorski J, Klimas K, Krauze T, Marciniak R, et al. Sex differences in excess and reservoir arterial blood pressures as markers of phenotype. J Hypertens. 2019;37:2159–67.
2. Song JJ, Ma Z, Wang J, Chen LX, Zhong JC. Gender differences in hypertension. J Cardiovasc Transl Res. 2020;13:47–54.
3. Ramirez LA, Sullivan JC. Sex differences in hypertension: where we have been and where we are going. Am J Hypertens. 2018;31:1247–54.
4. Rauchova H, Hojna S, Kadlecova M, Vaneckova I, Zicha J. Sex differences in blood pressure of aged Ren-2 transgenic rats. Physiol Res. 2020;69:245–52.
5. Patrice C, Delpech R, Panjo H, Falcoff H, Saurel-Cubizolles MJ, Ringa V, et al. Differences based on patient gender in the management of hypertension: a multilevel analysis. J Hum Hypertens. 2021. https://doi.org/10.1038/s41371-20-00450. Online ahead of print.
6. Hinojosa-Laborde C, Craig T, Zheng W, Ji H, Haywood JR, Sandberg K. Ovariectomy augments hypertension in aging female Dahl salt-sensitive rats. Hypertension. 2004;44:405–9.
7. Li BY, Qiao GF, Feng B, Zhao RB, Lu YJ, Schild JH. Electrophysiological and neuroanatomical evidence of sexual dimorphism in aortic baroreceptor and vagal afferents in rat. Am J Physiol. 2008;295:R1301–10.
8. Li BY, Schild JH. Patch clamp electrophysiology in nodose ganglia of adult rat. J Neurosci Methods. 2002;115:157–67.
9. Li BY, Schild JH. Electrophysiological and pharmacological validation of vagal afferent fiber type of neurons enzymatically isolated from rat nodose ganglia. J Neurosci Methods. 2007;164:75–85.
10. Qiao GF, Li BY, Lu YJ, Fu YL, SChild JH. 17Beta-estradiol restores excitability of a sexually dimorphic subset of myelinated vagal afferents in ovariectomized rats. Am J Physiol Cell Physiol. 2009;297:C654–64.
11. Lu XL, Xu WX, Yan ZY, Qian Z, Xu B, Liu Y, et al. Subtype identification in acutely dissociated rat nodose ganglion neurons based on morphologic parameters. Int J Biol Sci. 2013;9:716–27.
12. Feng Y, Liu Y, Cao PX, Sun X, Li KX, Li XY, et al. Estrogen-dependent microRNA-504 expression and related baroreflex afferent neuroexcitation via negative regulation on KCNMB4 and KCa1.1 beta4-subunit expression. Neuroscience. 2020;442:168–82.
13. Santa Cruz Chavez GC, Li BY, Glazebrook PA, Kunze DL, Schild JH. An afferent explanation for sexual dimorphism in the aortic baroreflex of rat. Am J Physiol Heart Circ Physiol. 2014;307:H910–21.
14. Xu WX, Yu JL, Feng Y, Yan QX, Li XY, Li Y, et al. Spontaneous activities in baroreflex afferent pathway contribute dominant role in parasympathetic neurocontrol of blood pressure regulation. CNS Neurosci Ther. 2018;24:1219–30.
15. Liu Y, Zhou JY, Zhou YH, Wu D, He JL, Han LM, et al. Unique expression of angiotensin Type-2 receptor in sex-specific distribution of myelinated Ah-type baroreceptor neuron contributing to sex-dimorphic neurocontrol of circulation. Hypertension. 2016;67:783–91.
16. Liu Y, Wu D, Qu MY, He JL, Yuan M, Zhao M, et al. Neuropeptide Y-mediated sex- and afferent-specific neurotransmissions contribute to sexual dimorphism of baroreflex afferent function. Oncotarget. 2016;7:66135–48.
17. Yuan M, Ma MN, Wang TY, Feng Y, Chen P, He C, et al. Direct activation of tachykinin receptors within baroreflex afferent pathway and neurocontrol of blood pressure regulation. CNS Neurosci Ther. 2019;25:123–35.
18. Chen P, Xu B, Feng Y, Li KX, Liu Z, Sun X, et al. FGF-21 ameliorates essential hypertension of SHR via baroreflex afferent function. Brain Res Bull. 2020;154:9–20.
19. Liu Y, Zhao SY, Feng Y, Sun J, Lu XL, Yan QX, et al. Contribution of baroreflex afferent pathway to NPY-mediated regulation of blood pressure in rats. Neurosci Bull. 2020;36:396–406.
20. Li Y, Feng Y, Liu L, Li X, Li XY, Sun X, et al. The baroreflex afferent pathway plays a critical role in H2S-mediated autonomic control of blood pressure regulation under physiological and hypertensive conditions. Acta Pharmacol Sin. 2021;42:898–908.
21. Wen X, Yu X, Huo R, Yan QX, Wu D, Feng Y, et al. Serotonin-mediated cardiac analgesia via Ah-type baroreceptor activation contributes to silent angina and asymptomatic infarction. Neuroscience. 2019;411:150–63.
22. Li JN, Li XL, He J, Wang JX, Zhao M, Liang XB, et al. Sex- and afferent-specific differences in histamine receptor expression in vagal afferents of rats: a potential mechanism for sexual dimorphism in prevalence and severity of asthma. Neuroscience. 2015;303:166–77.
23. Li JN, Qian Z, Xu WX, Xu B, Lu XL, Yan ZY, et al. Gender differences in histamine-induced depolarization and inward currents in vagal ganglion neurons in rats. Int J Biol Sci. 2013;9:1079–88.
24. Hunsberger MS, Mynlieff M. BK potassium currents contribute differently to action potential waveform and firing rate as rat hippocampal neurons mature in the first postnatal week. J Neurophysiol. 2020;124:703–14.
25. Wu F, Sun H, Gong W, Li X, Pan Z, Shan H, et al. Genetic and pharmacological inhibition of two-pore domain potassium channel TREK-1 alters depression-related behaviors and neuronal plasticity in the hippocampus in mice. CNS Neurosci Ther. 2021;27:220–32.
26. Schild JH, Kunze DL. Differential distribution of voltage-gated channels in myelinated and unmyelinated baroreceptor afferents. Auton Neurosci. 2012;172:4–12.
27. Hay M, Kunze DL. Calcium-activated potassium channels in rat visceral sensory afferents. Brain Res. 1994;639:333–6.
28. Li BY, Glazebrook P, Kunze DL, Schild JH. KCa1.1 channel contributes to cell excitability in unmyelinated but not myelinated rat vagal afferents. Am J Physiol Cell Physiol. 2011;300:C1393–403.
29. Liu Y, Wen X, Liu SZ, Song DX, Wu D, Guan J, et al. KCa1.1-mediated frequency-dependent central and peripheral neuromodulation via Ah-type baroreceptor neurons located within nodose ganglia and nucleus of solitary tract of female rats. Int J Cardiol. 2015;185:84–7.
30. Zhang YY, Yan ZY, Qu MY, Guo XJ, Li G, Lu XL, et al. KCa1.1 is potential marker for distinguishing Ah-type baroreceptor neurons in NTS and contributes to sex-specific presynaptic neurotransmission in baroreflex afferent pathway. Neurosci Lett. 2015;604:1–6.
31. Yan ZY, He JL, Wen X, Zuo M, Guan J, Wu D, et al. Variations in afferent conduction and axonal morphometrics of aortic depressive nerve imply wider baroreflex function of low-threshold and sex-specific myelinated Ah-type baroreceptor neurons in rats. Int J Cardiol. 2015;182:23–6.
32. He JL, Li JN, Zuo CM, Wang LQ, Wen X, Zuo M, et al. Potentiation of 17beta-estradiol on neuroexcitability by HCN-mediated neuromodulation of fast-afterhyperpolarization and late-afterdepolarization in low-threshold and sex-

specific myelinated Ah-type baroreceptor neurons via GPR30 in female rats. Int J Cardiol. 2015;182:174–8.
33. Xu WX, Ban T, Wang LQ, Zhao M, Yin L, Li G, et al. KCa1.1 beta4-subunits are not responsible for iberiotoxin-resistance in baroreceptor neurons in adult male rats. Int J Cardiol. 2015;178:84–7.
34. Wladyka CL, Feng B, Glazebrook PA, Schild JH, Kunze DL. The KCNQ/M-current modulates arterial baroreceptor function at the sensory terminal in rats. J Physiol. 2008;586:795–802.
35. Huo R, Xu WX, Han LM, He JL, Liu Y, Lu XL, et al. Fine tuning of calcium on membrane excitation of baroreceptor neurons in rats. Int J Cardiol. 2014;174:883–7.